Developmental timing scales wing patterning between avian species

Holly Stainton and Matthew Towers*

Department of Biomedical Science, University of Sheffield, Western Bank, Sheffield, S10 2TN, UK

* E-mail m.towers@sheffield.ac.uk

How development is timed between differently sized species is a fundamental question in biology. To address this problem, we compared wing development in the quail and the larger chick. We reveal that developmental timing is faster in the quail than in the chick, and is associated with pattern specification, proliferation, organiser duration, differentiation and apoptosis. However, developmental timing is independent of the growth rate, which is equivalent between both species, and therefore scales pattern to the size of the wing. We reveal that developmental timing can be either maintained or reset in interspecies tissue grafts, and we implicate retinoic acid as the resetting signal. Accordingly, retinoic acid can switch species developmental timing and rescale pattern, both between the quail and chick, and the chick and the larger turkey. We suggest that the scaling of pattern to wing bud size is achieved by the modulation of developmental timing against a comparable rate of growth.

Summary - We show that developmental timing scales wing patterning

Introduction

Although we know much about how the limb is patterned, we know little about how this process is timed between differently sized species. The avian wing provides an excellent system to understand this problem, as we possess in-depth knowledge of the underlying developmental patterning mechanisms that rely on the integration of extrinsic signalling and autonomous timing processes [1]. Thus, the embryonic development of the chick wing involves a switch from proximal signalling from the body wall (humerus/stylopod specification) to an autonomous timing mechanism operating in mesoderm cells at the distal tip of the outgrowing bud (digit/autopod specification) [2-7]. Recent evidence suggests that this transition from proximal signalling to autonomous timing occurs during forearm/zeugopod specification [2, 6, 8]. Retinoic acid emanating from the trunk of the embryo is considered to be involved in forelimb initiation, and is also implicated as the extrinsic signal involved in proximal specification [4, 5, 9-11]. Accordingly, specification of positional values that encode the different segments of the limb is associated with the progressive expression of genes encoding 5' Hox proteins: *Hoxa/d10* provides a read-out of stylopod specification, and then *Hoxa/d11* followed by *Hoxa/d13* provide read-outs of zeugopod and autopod specification, respectively [12, 13].

During proximo-distal development, complex reciprocal epithelio-mesodermal signalling interactions sustain limb outgrowth. The distal mesoderm maintains the overlying apical ectodermal ridge by producing a signal encoded by the Bmp inhibitor, *Gremlin1* [14-16]. The apical ectodermal ridge is a thickening of the distal epithelium that maintains limb outgrowth [17-20] and is marked by the expression of *Fgf8*. However, the proliferative growth of the chick wing is an autonomous property of the mesoderm and is associated with the precise regulation of cell cycle parameters (G1-S-phase entry), in both the distal tip and in the polarising region [3, 21] – a region of posterior-distal mesoderm that produces Sonic hedgehog

(Shh), which is involved in specifying positional values along the antero-posterior axis (thumb to little finger) [22, 23]. Proximo-distal patterning is complete when the apical ectodermal ridge regresses after the skeleton has been laid down, as determined by the expression of *Sox9* in condensing cartilage cells [24].

Here we provide evidence that species-specific developmental timing scales avian wing patterning. We implicate retinoic acid as the signal that sets developmental timing, which is accelerated in the wings of smaller species. We propose that retinoic acid signalling scales avian wing patterning by offsetting developmental timing against a comparable rate of growth.

Results

Developmental timing is accelerated in the quail compared to the chick

To understand how patterning is timed between differently sized species, we analysed wing development in the quail in reference to the Hamburger Hamilton (HH) staging system of the larger chick (Fig. 1a-c). The quail and chick are both in the Galliformes order and have incubation periods of 16 and 21 days, respectively. At day 3 of incubation, quail and chick embryos are at an equivalent stage (HH18/19), as determined by the appearance of the allantois (extra-embryonic membrane sac) and somites extending into the tail bud (approximately 36 pairs) [25-27]. At this stage, the chick embryo is slightly wider than the quail (between the wing buds), but it is not significantly different in length (from the tail bud to metencephalon – Supp Fig. 1). At HH18/19, wing buds can be identified as slight symmetrical bulges protruding from the flank of the embryo (0-hours, as defined by the last time-point that quail and chick wings are at an equivalent stage of development Fig. 1b,c). The full pattern of skeletal elements is laid down by HH29 when the apical ectodermal ridge regresses, which the chick wing bud

reaches at 72 hours, compared to 60 hours in the quail wing bud (Fig 1b,c). Correspondingly, *Fgf8* is expressed in the apical ectodermal ridge for an equivalent duration, which is therefore 12 hours shorter in the quail wing (Fig. 1d). Similarly, there is a 12-hour difference in the timing of *Sox9* expression, which is a marker of differentiating chondrogenic cells that prefigure the entire skeletal pattern by HH29 [24, 28]. Thus, the onset of *Sox9* expression occurs at HH22 in both species, and this 12-hour difference in timing can be appreciated by its similar spatial pattern at HH27/28, which is reached at 48 hours in the quail and 60 hours in the chick (Fig. 1e). To further assess the timing of development, we analysed the anterior and posterior necrotic zones, which are regions of apoptosis in the developing wing [29, 30]. As with the apical ectodermal ridge and differentiating chondrogenic cells, there is a 12-hour difference in the timing of apoptosis between quail and chick wings. Thus, the anterior necrotic zone persists between HH26 and HH27/28 and the posterior necrotic zone is detected at HH30 in both species (Fig. 1f).

Taken together, these findings reveal that developmental timing is accelerated in the quail wing bud by HH22, and this results in patterning being completed 12 hours earlier than it is in the chick wing.

Developmental timing scales patterning to the size of the wing

Having shown that pattern formation is completed 12 hours earlier in the quail compared to the chick, we determined how this process is scaled to the size of the wing by measuring incremental growth rates. Between 0 and 12 hours, quail wings buds grow at a significantly faster rate than chick wings buds and therefore become significantly longer along the proximo-distal axis (Fig. 2a). However, after 12 hours, their incremental growth rates are not significantly different up until the last time-point measured at 72 hours (HH30 in quail

wings that are 3.7mm in length, HH29 in chick wings that are 3.5mm – Fig. 2a). Therefore, the developmental progression through HH stages becomes uncoupled from the comparable rate of incremental growth between quail and chick wings. This can be appreciated by the observation that growth rates plateau between 48 and 60 hours in both species, although this occurs between different HH stages (HH27/28-HH29 in quail and HH26-HH27/28 in chick – Fig. 2a). A notable observation is that when the complete proximo-distal skeletal pattern is laid down at HH29 (chick 72 hours, quail 60 hours – Fig. 1e), it is scaled to the size of the wing (1.34-fold longer in the chick compared to the quail – Fig. 2b).

These data show that the quail and chick wing have comparable rates of growth, which become offset from species developmental timing (Fig. 2a), This results in pattern formation being scaled to the size of the wing, which is smaller in the quail.

Proliferation is linked with developmental timing and is independent of wing growth rate

To determine if changes in the rate of proliferation could account for the similar growth rates of quail and chick wings, we used flow cytometry to determine the proportion of distal mesoderm cells in G1-phase of the cell cycle [2, 21]. Although most cells in the early wing bud are dividing, cells in the undifferentiated distal mesoderm provide an accurate indicator of the diminishing rate of cell proliferation during the patterning phase [2, 21]. Analyses of the data reveal that cell proliferation rates do not correlate with the growth plateau that occurs between 48 and 60 hours in both species (Fig. 2c). By contrast, significant changes in proliferation rate correlate better with the timing of HH stage progression, which can be appreciated by the acute increase in the percentage of G1-phase cells (indicative of a decreasing proliferation rate) at HH27/28 in both species (Fig. 2c - 48 hours in the quail and 60 hours in the chick). Therefore,

cell proliferation is associated with developmental timing and is unlikely to account for major differences in the rate of proximo-distal elongation between quail and chick wings.

Proximo-distal specification is faster in quail wings compared to chick wings

To investigate if the 12-hour difference in developmental timing between quail and chick wings is associated with proximo-distal positional value specification, we analysed 5' *Hox* expression. The switch from proximal specification (stylopod) to intermediate specification (zeugopod) is indicated by the activation of *Hoxa11* expression, and the switch from intermediate specification (zeugopod) to distal specification (autopod) is indicated by the activation of *Hoxa13* expression [2, 8, 13, 31]. Expression of *Hoxa11* is detectable in the quail wing bud at 6 hours and in the chick at 12 hours (Fig. 3a, HH20/21 in both cases), which resolves into a 12-hour difference in timing at later stages (compare 48-hour quail to 60-hour chick). By contrast, expression of *Hoxa13* is detectable in the quail wing bud at 12 hours and in the chick at 24 hours (Fig. 3b, HH22 in both cases), and this 12-hour difference in timing is maintained throughout outgrowth. Thus, the switch from stylopod to zeugopod specification occurs 6 hours later in the chick wing bud compared to the quail, and the switch from zeugopod to autopod specification occurs 12 hours later. An interesting observation from our growth curve (Fig. 2a) and proximo-distal specification timing data is that the size ratio between quail and chick wing buds when *Hoxa13* is activated at HH22, is comparable to those observed when the pattern of skeletal elements has been laid down at HH29 (Fig. 2b).

Taken together, these findings reveal that proximo-distal positional value specification is accelerated by 12 hours in the quail wing bud compared to the chick. In addition, because proximo-distal positional value specification is offset from growth between the two species,

this means that it is scaled to the size of the wing bud and anticipates the size of the complete pattern produced at HH29.

Stability and resetting of developmental timing in interspecies grafts

To understand how the 12-hour difference in developmental timing is set between quail and chick wings, we performed a series of reciprocal tissue grafting experiments to ascertain if it is reset or maintained. We chose the polarising region, as it expresses *Sonic hedgehog* (*Shh)* and regulates its cell cycle parameters for an autonomously defined duration in the chick wing [7, 32]. Indeed, as we observed with *Hoxa11/13* expression (Fig. 3a,b) and with the acquisition of morphological landmarks (Fig. 1, 2), there is a 12-hour difference in the developmental timing of *Shh* expression in quail and chick wings. Thus, *Shh* expression persists for 36 hours in the quail wing and for 48 hours in the chick (until HH26 in both species, Fig. 4a).

We performed interspecies polarising region grafts to the anterior margins of host wing buds at 12 hours when developmental timing is accelerated in the quail compared to chick (HH21 chick and HH22 quail – Fig. 4b,d, note that stage-matched intraspecies control grafts maintain their normal duration of *Shh* expression – Supp Fig. 2). We found that grafts performed at these stages maintain their species timing of *Shh* expression. Thus, at 48 hours, *Shh* expression is undetectable in quail cells grafted to a chick wing, but is detectable in the host (Fig. 4c). In the reciprocal experiment, *Shh* expression is detectable in chick cells grafted to a quail wing, but is undetectable in the host (Fig. 4e). In addition, both grafted quail and chick wing bud polarising region cells maintain species-specific cell cycle parameters typical of their donor age (Fig. 4f; 63.3% G1-phase cells in quail graft vs. 71% in chick host; 72.6 chick graft vs. 64% in quail host). Rather than being an autonomous process, it has also been

suggested that the termination of *Shh* expression requires the displacement of *Gremlin1*-expressing cells by a critical distance from the polarising region in order to break down a self-propagating extrinsic signalling loop [33]. However, in chick wings that received quail polarising region grafts, *Shh* expression is terminated in donor cells independently of their proximity to the duplicate domain of *Gremlin1* expression in the host (Supp Fig. 3). Thus, these findings show that the species timing of both *Shh* expression and cell cycle parameters are autonomously determined after HH21.

We also performed interspecies polarising region grafts at 0 hours when developmental timing is equivalent in chick and quail wing buds (HH18/19 - Fig. 4g,i). Unlike with the 12-hour grafts, *Shh* expression is reset to the host duration in 0-hour interspecies grafts. Thus, at the 48-hour time-point, *Shh* expression duration is prolonged in quail cells in a chick wing, and is prematurely terminated in chick cells in a quail wing (Fig. 4h,j, respectively - note that 0-hour intraspecies control grafts maintain their normal duration of *Shh* expression - Supp Fig. 3). In addition, cell cycle parameters are also reset close to host values in both grafted quail and chick wing bud polarising regions (Fig. 4k; 59% G1-phase cells in quail graft vs. 60% in chick host; 54% in chick graft vs. 56% in quail host).

These results reveal that the species timing of both *Shh* expression and cell cycle parameters are autonomously maintained in 12-hour polarising region grafts when developmental timing has become offset between the quail and chick (HH21 vs. HH22), but that they can be reset in 0-hour grafts when developmental timing is equivalent (HH18/19).

Retinoic acid can reset the species-specific timing of *Shh* expression

Since the developmental timing of *Shh* expression can be reset by the host environment in interspecies polarising region grafts performed at 0 hours, but not at 12 hours, this suggests

the existence of a resetting signal. Retinoic acid is the only known signal in the chick wing bud that, although present at high-levels at 0 hours (HH18/19), is cleared from the distal region of the wing bud by 12 hours (HH21) [10, 34-36], as indicated by its downstream transcriptional target *Meis1*, and the up-regulation of the gene encoding the retinoic acid degrading enzyme, Cyp26b1[6, 37] (Supp Fig. 4). The loss of distal *Meis1* expression occurs earlier in the quail wing bud at approximately 6 hours, compared to 12 hours in the chick wing bud (Supp Fig. 4a – HH20/21 in both species). However, as with 5' *Hox* gene expression, the spatial expression of *Meis1* resolves into a 12-hour difference by HH22, which is reached at 24 and 36 hours in quail and chick wing buds, respectively (Supp Fig. 4a). Additionally, between 0-12 hours of wing bud outgrowth, *Cyp26b1* levels rise significantly faster in the quail compared to the chick (Supp Fig. 4b). This indicates an increased rate of retinoic acid degradation in the wing buds of the smaller species.

The differences in the expression of genes that regulate and respond to retinoic acid signalling between quail and chick wing buds could suggest that it is a signal that sets developmental timing. Therefore, we asked if the transient maintenance of retinoic acid signalling by carrier beads for 12-20 hours in the chick wing bud [38, 39] would reverse the autonomy of *Shh* expression timing in quail polarising region grafts made to the chick wing at the 12-hour time-point (Fig. 5a). Indeed, by transiently prolonging retinoic acid signalling, *Shh* expression timing is reset in the quail polarising region graft, as it is maintained for approximately the same duration as is seen in the host chick polarising region (approx. 56 hours - Fig. 5b, compare with failure to reset timing in the same experiment minus retinoic acid - Fig, 4b, c). It is worth noting that the duration of *Shh* expression is also extended in the retinoic acid-treated host chick polarising region (compare to level of residual *Shh* expression in the

contralateral untreated chick wing bud in Fig. 5b). These observations show that retinoic acid can reset the species developmental timing of *Shh* expression.

Retinoic acid can set species developmental timing and rescale patterning

Having demonstrated that retinoic acid can reset the 12-hour difference in the species timing of *Shh* expression between the quail and chick, we questioned if it could have a general role in setting developmental timing. Indeed, when retinoic acid is applied on beads to HH18/19 quail and chick wing buds at 0 hours to transiently maintain it for 12-20 hours [38, 39], the subsequent progression through HH stages occurs approximately 12 hours later than normal, such that HH29 is reached at 72 hours and 84 hours, respectively (Fig. 5c,d,). Correspondingly, as predicted from the polarising region grafting experiments (Fig. 5a,b), retinoic acid extends the duration of *Shh* expression for 12 hours in both quail and chick wings (until 48 hours and 60 hours, respectively Fig. 5e), which is HH26 in both species (Fig. 5c). Likewise, retinoic acid delays zeugopod specification for 3 hours in chick wing buds and for 6 hours in quail wing buds (Fig. 5f – until HH20/21), and delays autopod specification for 12 hours in both species (Fig. 5g – until HH22). However, the incremental growth rates of retinoic acid-treated quail and chick wings are not significantly different from those of untreated controls (Fig. 5h). Therefore, when *Hoxa13* is activated at HH22, retinoic acid-treated quail wing buds are 1.26-fold longer than untreated controls, and retinoic acid-treated chick wing buds are 1.23-fold longer than untreated controls, meaning that pattern specification is scaled appropriately to the size of the wing bud (Supp Fig. 5) Similarly, when pattern formation is completed at HH29, retinoic acid-treated quail wings are 1.42-fold longer than untreated controls, and retinoic acid-treated chick wings are 1.46-fold longer than untreated controls (Supp Fig. 5). These results show that retinoic acid-treated quail wings and untreated chick

wings have equivalent developmental timing and growth rates. This results in pattern specification and subsequent pattern formation being equivalently scaled to the size of the wing.

Chick wings treated with retinoic acid mimic turkey developmental timing and pattern scaling

Having revealed that developmental timing is advanced by 12 hours in quail wings compared to chick wings, and that it is equivalent in retinoic acid-treated quail and chick wings (Figs 1, 5), we asked if retinoic acid-treated chick wings replicate timing found in a larger species. Therefore, we chose the turkey, which like the quail and chick, belongs to the Galliformes order (Fig. 6a –note the turkey has an incubation period of 28 days).

We staged turkey wings according to the HH staging system of the chick, starting at HH18/19, which is reached at day 4 of incubation (note that the quail and chick reach HH18/19 at day 3). At HH18/19 the turkey embryo is significantly longer than the quail, but not the chick (from the tail bud to metencephalon), and is similar in width to both quail and chick embryos (between the wing buds, Supp Fig. 6a,b). During the next 12 hours, turkey wing buds only progress to HH19/20, whereas chick wing buds reach HH20/21, and subsequently, HH stage progression resolves into a 12-hour difference between the two species by 48 hours. Thus, HH29 is reached in 84 hours in turkey wings compared to 72 hours and 60 hours for chick and quail wings, respectively (Fig. 6b,d). Therefore, both retinoic acid-treated chick wings and turkey wings require 12 hours longer than untreated chick wings to reach HH29 (Fig. 6b,d). Furthermore, turkey wings grow at a similar incremental rate along the proximo-distal axis compared to quail and chick wings - either untreated or treated with retinoic acid (Fig. 6c). Therefore, because growth is offset from developmental timing, pattern formation is scaled to

the size of the wing at HH29; thus, turkey wings are 1.31-fold longer chick wings and, similarly retinoic acid-treated chick wings that are 1.46-fold longer than chick wings. (Supp Fig. 6c)

To investigate developmental timing further in the turkey wing, we analysed the expression of *Shh,* and found that transcripts can be detected for 60 hours (until HH26) in turkey wings (Fig. 6e). This is comparable to the duration of *Shh* expression in retinoic acid-treated chick wing buds (Fig. 5e), which is 12 hours longer than is found in untreated chick wings (48 hours – Fig. 4a). Furthermore, we determined the timing of proximo-distal specification in turkey wing buds, by analysing 5' *Hox* expression. The onset of *Hoxa11* expression (zeugopod specification) occurs at 18 hours (HH20/21), and *Hoxa13* expression (autopod specification) at 30 hours (HH22) (Fig. 6f,g, respectively), which are comparable timings to those found in retinoic acid-treated chick wing buds (Fig. 5f,g). Combining this data with our growth curve data (Fig. 6c) reveals that the size of the wing bud is comparably scaled between chicks and retinoic acid-treated chicks, and also between chicks and turkeys when *Hoxa13* is initiated at HH22 (1.24-fold and 1.23-fold different, respectively - Supp Fig 6c).

Taken together, these findings reveal that retinoic acid-treated chick wings and turkey wings have equivalent developmental timing and rates of growth. This results in the equivalent scaling of pattern specification and pattern formation.

Discussion

We have presented a new mechanism to explain how the wing pattern is scaled between different avian species (Fig. 7). The rate of growth is not significantly different between the wings of different avian species. However, the tempo of proximo-distal specification and the subsequent timing of patterning events is variable. Consequently, this scales proximo-distal pattern to the size of the wing (Fig. 7). We implicated retinoic acid as the signal that sets the

tempo of proximo-distal specification. Accordingly, transiently prolonging retinoic acid signalling results in the quail wing having equivalent developmental timing to the chick wing, and thus, equivalently scaled skeletal patterns. We also showed that the same procedure in the chick wing mimics developmental timing and pattern scaling found in the turkey wing.

Avian wing developmental timing

We revealed that the timing of proximal-distal specification is variable in the wing buds of different avian species. For instance, there is an 18-hour difference in the onset of *Hoxa13* expression that marks the transition from zeugopod to autopod specification between quail and turkey wing buds. However, we are unable to determine when proximo-distal specification is complete, because *Hoxa13* continues to be expressed at least until day 10 of incubation [(2)]. Recent findings invite speculation into the underlying mechanism that could determine the species duration of proximo-distal specification. It is suggested that the degradation of a proximal signal, considered to be retinoic acid, is interpreted into a gradient of Meis1/2 protein abundance [(8)]. Opposing Fgf signals from the apical ectodermal ridge also influence the distribution of retinoic acid signalling [(8, 9, 37)]. In this model, high Meis1/2 levels specify stylopod positional values; low Meis1/2 zeugopod positional values, and absent Meis1/2 autopod positional values. The predicted distribution of retinoic acid does not appear to be influenced by the size of the embryo, because the quail, chick and turkey have similar trunk widths. However, our data indicate a role for the retinoic acid degrading enzyme, Cyb26b1, in timing the removal of retinoic acid between quail and chick wing buds. Thus, *Cyp26b1* expression in the quail wing bud increases at a significantly faster rate over time compared to the chick, suggesting an earlier loss of retinoic acid in the smaller species. Therefore, a potential pattern specification scaling mechanism could involve species-specific retinoic acid

degradation rates in determining the timing of proximo-distal specification. In a similar manner, the rate of protein degradation in cultured mouse cells is approximately twice as fast as is found in human cells, which correlates with the tempo of somitogenesis and motor neuron differentiation [40, 41]. It remains to be determined if altering the degradation of specific signalling molecules and/or proteins is sufficient to switch human and mouse developmental timing, and if this has implications for in vivo tissue scaling.

Autopod specification is also controlled by an autonomous epigenetic mechanism, which means that *Hoxa13* expression cannot be precociously activated by the removal of retinoic acid signalling [2, 6, 8]. It is also possible that another signal works in parallel with retinoic acid, and supplements its function when removed. Therefore, we have been unable to determine if patterning can be rescaled from large to small species. Our reciprocal polarising region grafting experiments between the quail and chick also confirm that the autonomous development of the wing coincides with the loss of retinoic acid signalling and the onset of autopod specification. Thus, grafts performed at this stage maintain their species duration of *Shh* expression, irrespective of the extrinsic signalling environment, which was predicted to be the key parameter in previous work [32]. Consistent with these observations, *Shh* expression is reset to the duration of the host species in grafts performed at earlier stages.

We revealed that the timing of proximal-distal specification varies between the wing buds of different avian species. However, following proximo-distal specification, the autonomously timed programme of distal development then continues at a similar tempo and duration in both quail and chick wings, until patterning is complete (Fig. 7). This can be appreciated by the similar timings of a series of morphological, cellular and molecular landmarks including proliferation rates, differentiation, apoptosis and organiser duration. For

instance, there is only a 6-hour difference in the time taken from the onset of *Hoxa13* expression and the regression of the apical ectodermal ridge in quail and turkey wings (Fig. 7). Although, because the timing of proximo-distal specification varies significantly between different species, it has dramatic effects on organiser duration. Thus, both the polarising region and apical ectodermal ridge persist for 24 hours longer in turkey wings compared to quail wings. An interesting avenue of research will be to explore if the duration of other embryonic organisers is linked to pattern specification.

It remains unclear how the intrinsically timed events involved in the development of the distal part of the wing are integrated once *Hoxa13* is activated. One possibility is that the cell cycle constitutes an overarching developmental timing mechanism, because it is intimately coupled with differentiation and apoptosis. Accordingly, mesodermal cell proliferation in the chick wing is linked to the duration of the polarising region [7, 32] and the apical ectodermal ridge [21]. Indeed, evidence that the cell cycle could act as a developmental timer arises from the similarities between chick wing development and cultured oligodendroctye progenitor cell development. In both cases, retinoic acid is implicated in triggering the onset of a cell cycle timer that involves the progressive lengthening of the G1-phase of the cell cycle [32, 42-44], and is associated with the activation of D-cyclin-dependent kinase inhibitors, which are important negative regulators of the G1-S phase transition [7, 44].

Avian wing growth

A simple way in which pattern could be scaled between species is that it is specified over similar-sized domains, followed by differential growth [27, 45, 46]. However, an unexpected finding from our study is that the rate of growth is comparable between quail, chick and turkey wings, and is therefore uncoupled from species developmental timing. As a consequence,

proximo-distal specification is scaled to the size of the wing bud. For instance, at the onset of autopod specification - as determined by *Hoxa13* expression - there is a 1.57-fold difference in the length of the quail and turkey wing bud at HH22. Moreover, quail wings reach the end of the patterning phase at HH29 12 hours earlier than chick wings, and 24 hours earlier than turkey wings. As this occurs alongside a comparable growth rate between species, this results in a 1.8-fold difference in the length of the fully patterned quail and turkey wing at HH29 (Fig. 7). An implication of this finding is that proximo-distal pattern specification involves the scaling of the predicted anti-parallel retinoic acid and Fgf gradients to the size of the wing bud between different avian species[8]. Similarly, during neural tube patterning, progenitor domains are also scaled between different sized species[47], but this is due to the response of cells to Shh, rather than to changes in the Shh protein gradient itself.

We also showed that the proliferation rate of distal mesoderm cells is linked to proximo-distal developmental timing during the patterning phase. However, the mesodermal cell proliferation rate does not influence major changes in growth between different species. This finding fits with previous experimental observations in which the manipulation of proliferation failed to affect overall organ size [48-50]. These considerations could suggest that the growth of avian wings is controlled by a global mechanism, such as metabolism/nutrition, which regulates the Insulin/Insulin-like-1 Growth Factor (IGF/IGF-like-1) mTOR axis [50, 51]. Indeed, consistent with this hypothesis, components of this pathway are expressed in chick wing buds [52, 53], and *in vitro* studies have implicated a role for IGF in promoting limb outgrowth [54, 55].

Finally, the widespread distribution of retinoic acid in the embryo could suggest that it has a general role in co-ordinating developmental timing and pattern scaling. For instance, retinoic acid promotes the expression of anterior *Hoxb* genes along the main body axis and needs to be removed by Cyp26b1 to permit the expression of posterior *Hoxb* genes[56]. Thus,

the relative timing of *Hoxb* expression is suggested to underlie changes in avian limb position that have occurred during evolution [56, 57]. However, it remains to be determined if retinoic acid globally affects developmental timing independently of the growth along the main body axis, as we suggest it does in the limb. Nevertheless, these considerations could suggest that retinoic acid coordinates limb positioning with limb pattern scaling by controlling developmental timing.

Methods

Avian husbandry and wing measurements

Bovans Brown chicken eggs (*Gallus gallus domesticus*), Japanese quail eggs (*Coturnix japonica*), and Bronze turkey eggs (*Meleagris gallopavo domesticus*) were incubated at 37°C and staged according to the Hamburger Hamilton staging system [30] based on the number of somites present, and by characteristic morphological features of the wing bud. HH18/19 is reached by incubation day 3 in quails and chicks, and day 4 in turkeys, and is referred to in this study as 0 hours of wing outgrowth. Embryos of the appropriate age were dissected in PBS and measurements of the proximo-distal axis were taken down the centre of the limb bud, from the proximal boundary of the limb with the body wall, to the distal tip of the limb bud, accounting for elbow bend where appropriate.

Whole mount *in situ* hybridisation

Embryos were fixed in 4% PFA overnight at 4°C then dehydrated in methanol overnight at −20°C. Embryos were then rehydrated through a methanol/PBS series, washed in PBS, then treated with proteinase K for 20 mins (10 $\mu g/ml^{-1}$), washed in PBS, fixed for 30 mins in 4% PFA at room temperature and then prehybridised at 67°C for 2 hours (50% formamide/50% 2x SSC). 1 µg of antisense DIG-labelled mRNA probes were added to 1 ml of hybridisation buffer (50% formamide/50% 2x SSC) at 67°C overnight. Embryos were washed twice in hybridisation buffer, twice in 50:50 hybridisation buffer and MAB buffer, and then twice in MAB buffer, before being transferred to blocking buffer (2% blocking reagent 20% foetal bovine serum in MAB buffer) for 3 hours at room temperature. Embryos were transferred to blocking buffer containing anti-digoxigenin antibody (1:2000) at 4°C overnight, then washed

in MAB buffer overnight before being transferred to NTM buffer containing NBT/BCIP and mRNA distribution visualised using a LeicaMZ16F microscope.

Flow cytometry

Polarising regions or distal mesenchyme pooled from 8-12 replicate experiments were dissected in PBS under a LeicaMZ16F microscope using fine surgical scissors, and digested into single cell suspensions with trypsin (0.05%, Gibco) for 30 mins at room temperature. Cells were briefly washed in PBS, fixed in 70% ethanol overnight, washed in PBS and re-suspended in PBS containing 0.1% Triton X-100, 50 $\mu g/ml^{-1}$ of propidium iodide and 50 $\mu g/ml^{-1}$ of RNase A (Sigma). Dissociated cells were left at room temperature for 20 mins, cell aggregates were removed by filtration and single cells analysed for DNA content with a FACSCalibur flow cytometer and FlowJo software (Tree star Inc.). Based on ploidy values cells were assigned G1, S, or G2/M phases, and this was expressed as a percentage of the total cell number (5,000–12,000 cells in each case). Statistical significance of numbers of cells in different phases of the cell cycle (G1 vs. S, G2 and M) between pools of dissected wing bud polarising region tissue (12–15 in each pool) was determined by Pearson's χ^2 tests to obtain two-tailed *P*-values (significantly different being a *p*-value of less than 0.05 – as in [32]). Statistical comparisons of cell cycle parameters between the wing buds of different species were compared using unpaired students *t*-tests to obtain a *p*-value.

Apoptosis analysis

Whole chick and quail wing buds were dissected in PBS and transferred to Lysotracker (Life Technologies, L-7528) PBS solution (1:1000) in the dark pre-warmed to 37°C. Wing buds

were incubated for 1 hour at 37°C, washed in PBS, and fixed overnight in 4% PFA at 4°C. Wing buds were then washed in PBS and progressively dehydrated through a methanol series.

Polarising region grafts

Polarising region grafts were performed as described in [58]. Briefly, donor embryos were dissected in PBS and the polarising regions removed using sharpened tungsten needles then transferred to the host embryo where they were grafted to equivalently sized regions of the host anterior limb bud and held in place with 25µm diameter platinum pins.

Quantitative PCR (qPCR)

Ten whole limb buds at 0, 6, 12 and 24 hours were dissected from either quail or chick embryos. Total RNA was extracted using TRIzol Reagent (Life Technologies), purified using a Direct-zol RNA kit (Zymo Research) and cDNA prepared using SuperScript III Reverse Transcriptase (Invitrogen). qPCR was performed on an Applied Biosystems StepOne RTPCR machine using SYBR Green Master Mix (Thermo Fisher Scientific) and a primer set for *Cyp26b1* was designed against a sequence which was present in both chicken and quails, spanning exon junctions (Thermo Fisher Scientific). 5 ng cDNA was used per reaction (20µl volume) with cycle conditions of 95 °C for 20 sec, followed by 32 cycles of 95 °C for 1 sec and 60 °C for 20 sec. All reactions were carried out in triplicate and average C_T values normalized against Eukaryotic *18S rRNA* Endogenous Control expression (Thermo Fisher Scientific). Unpaired student *t*-tests compared the mean relative expression, and measured significance of expression change between appropriate samples. Applied Biosystems StepOne Software V2.3 was used to analyse the data and GraphPad Prism8 used to construct graphs.

Bead implantation

Sieved AGX1-2 beads (150 or 200 μm in diameter, Sigma) were soaked in a stable form of all-*trans*-retinoic acid, TTNPB (Sigma, 0.05 mg/ml dissolved in DMSO, also Sigma) for 1 hour and then washed in DMEM before being grafted to the middle of wing buds using a sharp tungsten needle. TTNPB has been shown to diffuse from AGX1-2 beads over an approximate 12-20-hour period and can be used to model RA distribution in chick wing buds due to comparable patterning effects, kinetics and diffusion constants [35, 38, 39].

Data availability statement

The authors declare that the data supporting the findings of this study are available within the paper and its supplementary information files. Original data files including gating strategy related to the flow cytometry data in figure 1 and 4 can be found in Data S1 (flow cytometry source data) in the supplementary information file.

References

1. McQueen C, Towers M. Establishing the pattern of the vertebrate limb. Development. 2020;147(17):dev177956.

2. Saiz-Lopez P, Chinnaiya K, Campa VM, Delgado I, Ros MA, Towers M. An intrinsic timer specifies distal structures of the vertebrate limb. Nature communications. 2015;6.

3. Saiz-Lopez P, Chinnaiya K, Towers M, Ros MA. Intrinsic properties of limb bud cells can be differentially reset. Development. 2017;144(3):479-86.

4. Rosello-Diez A, Ros MA, Torres M. Diffusible signals, not autonomous mechanisms, determine the main proximodistal limb subdivision. Science. 332. United States2011. p. 1086-8.

5. Cooper KL, Hu JK, ten Berge D, Fernandez-Teran M, Ros MA, Tabin CJ. Initiation of proximal-distal patterning in the vertebrate limb by signals and growth. Science. 2011;332(6033):1083-6.

6. Rosello-Diez A, Arques CG, Delgado I, Giovinazzo G, Torres M. Diffusible signals and epigenetic timing cooperate in late proximo-distal limb patterning. Development. 141. England2014. p. 1534-43.

7. Pickering J, et al. An autoregulatory cell cycle timer integrates growth and specification in chick wing digit development. eLife. 2019;8:e47625.

8. Delgado I, López-Delgado AC, Roselló-Díez A, Giovinazzo G, Cadenas V, Fernández-de-Manuel L, et al. Proximo-distal positional information encoded by an Fgf-regulated gradient of homeodomain transcription factors in the vertebrate limb. Science Advances. 2020;6(23):eaaz0742.

9. Mic FA, Sirbu IO, Duester G. Retinoic acid synthesis controlled by Raldh2 is required early for limb bud initiation and then later as a proximodistal signal during apical ectodermal ridge formation. J Biol Chem. 279. United States2004. p. 26698-706.

10. Mercader N, Leonardo E, Piedra ME, Martinez AC, Ros MA, Torres M. Opposing RA and FGF signals control proximodistal vertebrate limb development through regulation of Meis genes. Development. 2000;127(18):3961-70.

11. Feneck E, Logan M. The Role of Retinoic Acid in Establishing the Early Limb Bud. Biomolecules. 2020;10(2).

12. Wellik DM, Capecchi MR. Hox10 and Hox11 genes are required to globally pattern the mammalian skeleton. Science. 2003;301(5631):363-7.

13. Nelson CE, Morgan BA, Burke AC, Laufer E, DiMambro E, Murtaugh LC, et al. Analysis of Hox gene expression in the chick limb bud. Development. 1996;122(5):1449-66.

14. Khokha MK, Hsu D, Brunet LJ, Dionne MS, Harland RM. Gremlin is the BMP antagonist required for maintenance of Shh and Fgf signals during limb patterning. Nature Genetics. 2003;34(3):303-7.

15. Laufer E, Nelson CE, Johnson RL, Morgan BA, Tabin C. Sonic hedgehog and Fgf-4 act through a signaling cascade and feedback loop to integrate growth and patterning of the developing limb bud. Cell. 79. United States1994. p. 993-1003.

16. Zuniga A, Haramis AP, McMahon AP, Zeller R. Signal relay by BMP antagonism controls the SHH/FGF4 feedback loop in vertebrate limb buds. Nature. 1999;401(6753):598-602.

17. Saunders J. The proximo-distal sequence of origin of the
parts of the chick wing and the role of the ectoderm. *Journal of Experimental Zoology Part A: Ecological and Integrative Physiology*1948. p. 363-403.

18. Summerbell D, Lewis JH, Wolpert L. Positional information in chick limb morphogenesis. Nature. 1973;244(5417):492-6.

19. Moon AM, Capecchi MR. Fgf8 is required for outgrowth and patterning of the limbs. Nat Genet. 2000;26(4):455-9.

20. Mahmood R, Bresnick J, Hornbruch A, Mahony C, Morton N, Colquhoun K, et al. A role for FGF-8 in the initiation and maintenance of vertebrate limb bud outgrowth. Current Biology. 1995;5(7):797-806.

21. Pickering J, Rich CA, Stainton H, Aceituno C, Chinnaiya K, Saiz-Lopez P, et al. An intrinsic cell cycle timer terminates limb bud outgrowth. Elife. 2018;7.

22. Tickle C, Towers M. Sonic Hedgehog Signaling in Limb Development. Front Cell Dev Biol. 2017;5:14.

23. Riddle RD, Johnson RL, Laufer E, Tabin C. Sonic hedgehog mediates the polarizing activity of the ZPA. Cell. 75. United States1993. p. 1401-16.

24. Healy C, Uwanogho D, Sharpe PT. Regulation and role of Sox9 in cartilage formation. Dev Dyn. 215. United States1999. p. 69-78.

25. Padgett CS, Ivey WD. The normal embryology of the Coturnix quail. Anat Rec. 1960;137:1-11.

26. Hamburger V, Hamilton HL. A series of normal stages in the development of the chick embryo. Dev Dyn. 1951;195(4):231-72.
27. Ainsworth SJ, Stanley RL, Evans DJ. Developmental stages of the Japanese quail. J Anat. 2010;216(1):3-15.
28. Pechak DG, Kujawa MJ, Caplan AI. Morphological and histochemical events during first bone formation in embryonic chick limbs. Bone. 7. United States1986. p. 441-58.
29. Fernandez-Teran MA, Hinchliffe JR, Ros MA. Birth and death of cells in limb development: a mapping study. Dev Dyn. 2006;235(9):2521-37.
30. Saunders JW, Jr., Gasseling MT. Cellular death in morphogenesis of the avian wing. Dev Biol. 5. United States1962. p. 147-78.
31. Vargesson N, Kostakopoulou K, Drossopoulou G, Papageorgiou S, Tickle C. Characterisation of hoxa gene expression in the chick limb bud in response to FGF. Dev Dyn. 2001;220(1):87-90.
32. Chinnaiya K, Tickle C, Towers M. Sonic hedgehog-expressing cells in the developing limb measure time by an intrinsic cell cycle clock. Nature Communications. 2014;5.
33. Scherz PJ, Harfe BD, McMahon AP, Tabin CJ. The limb bud Shh-Fgf feedback loop is terminated by expansion of former ZPA cells. Science. 305. United States2004. p. 396-9.
34. Thaller C, Eichele G. Identification and spatial distribution of retinoids in the developing chick limb bud. Nature. 1987;327(6123):625-8.
35. Eichele G, Thaller C. Characterization of concentration gradients of a morphogenetically active retinoid in the chick limb bud. J Cell Biol. 1987;105(4):1917-23.
36. Probst S, Kraemer C, Demougin P, Sheth R, Martin GR, Shiratori H, et al. SHH propagates distal limb bud development by enhancing CYP26B1-mediated retinoic acid clearance via AER-FGF signalling. Development. 2011;138(10):1913-23.
37. Yashiro K, Zhao X, Uehara M, Yamashita K, Nishijima M, Nishino J, et al. Regulation of retinoic acid distribution is required for proximodistal patterning and outgrowth of the developing mouse limb. Dev Cell. 6. United States2004. p. 411-22.
38. Eichele G, Tickle C, Alberts BM. Studies on the mechanism of retinoid-induced pattern duplications in the early chick limb bud: temporal and spatial aspects. J Cell Biol. 1985;101(5 Pt 1):1913-20.

39. Eichele G, Tickle C, Alberts B. Microcontrolled release of biologically active compounds in chick embryos: Beads of 200-µm diameter for the local release of retinoids. Analytical Biochemistry. 1984;142(2):542 - 55.

40. Matsuda M, Hayashi H, Garcia-Ojalvo J, Yoshioka-Kobayashi K, Kageyama R, Yamanaka Y, et al. Species-specific segmentation clock periods are due to differential biochemical reaction speeds. Science. 2020;369(6510):1450-5.

41. Rayon T, Stamataki D, Perez-Carrasco R, Garcia-Perez L, Barrington C, Melchionda M, et al. Species-specific pace of development is associated with differences in protein stability. Science. 2020;369(6510).

42. Durand B, Raff M. A cell-intrinsic timer that operates during oligodendrocyte development. Bioessays. 22. United States: 2000 John Wiley & Sons, Inc.; 2000. p. 64-71.

43. Gao FB, Durand B, Raff M. Oligodendrocyte precursor cells count time but not cell divisions before differentiation. Curr Biol. 1997;7(2):152-5.

44. Gao FB, Apperly J, Raff M. Cell-intrinsic timers and thyroid hormone regulate the probability of cell-cycle withdrawal and differentiation of oligodendrocyte precursor cells. Dev Biol. 197. United States: 1998 Academic Press.; 1998. p. 54-66.

45. Slack JM, Holland PW, Graham CF. The zootype and the phylotypic stage. Nature. 1993;361(6412):490-2.

46. Richardson MK. Heterochrony and the phylotypic period. Dev Biol. 172. United States1995. p. 412-21.

47. Uygur A, Young J, Huycke TR, Koska M, Briscoe J, Tabin CJ. Scaling Pattern to Variations in Size during Development of the Vertebrate Neural Tube. Dev Cell. 2016;37(2):127-35.

48. Day SJ, Lawrence PA. Measuring dimensions: the regulation of size and shape. Development. 2000;127(14):2977-87.

49. Conlon I, Raff M. Size control in animal development. Cell. 1999;96(2):235-44.

50. Crickmore MA, Mann RS. The control of size in animals: insights from selector genes. Bioessays. 2008;30(9):843-53.

51. Tumaneng K, Russell RC, Guan K-L. Organ size control by Hippo and TOR pathways. Current biology : CB. 2012;22(9):R368-R79.

52. McQueeney K, Dealy CN. Roles of insulin-like growth factor-I (IGF-I) and IGF-I binding protein-2 (IGFBP2) and -5 (IGFBP5) in developing chick limbs. Growth Horm IGF Res. 2001;11(6):346-63.

53. Allan GJ, Zannoni A, McKinnell I, Otto WR, Holzenberger M, Flint DJ, et al. Major components of the insulin-like growth factor axis are expressed early in chicken embryogenesis, with IGF binding protein (IGFBP) -5 expression subject to regulation by Sonic Hedgehog. Anat Embryol (Berl). 2003;207(1):73-84.

54. Sears KE, Patel A, Hubler M, Cao X, Vandeberg JL, Zhong S. Disparate Igf1 expression and growth in the fore- and hind limbs of a marsupial mammal (Monodelphis domestica). J Exp Zool B Mol Dev Evol. 2012;318(4):279-93.

55. Dealy CN, Kosher RA. IGF-I, insulin and FGFs induce outgrowth of the limb buds of amelic mutant chick embryos. Development. 1996;122(4):1323-30.

56. Moreau C, Caldarelli P, Rocancourt D, Roussel J, Denans N, Pourquie O, et al. Timed Collinear Activation of Hox Genes during Gastrulation Controls the Avian Forelimb Position. Curr Biol. 2019;29(1):35-50 e4.

57. Matsubara Y, Hirasawa T, Egawa S, Hattori A, Suganuma T, Kohara Y, et al. Anatomical integration of the sacral–hindlimb unit coordinated by GDF11 underlies variation in hindlimb positioning in tetrapods. Nature Ecology & Evolution. 2017;1(9):1392-9.

58. Stainton H, Towers M. Polarizing Region Tissue Grafting in the Chick Embryo Limb Bud. Methods Mol Biol. 2018;1863:143-53.

Acknowledgements: We acknowledge Cheryll Tickle and Marysia Placzek for critical reading

Funding: MT and HS the Wellcome Trust (202756/Z/16/Z)

Author contributions: HS performed and analysed the experiments and co-wrote the paper with MT who devised the study

The authors declare no competing interests

Correspondence and requests for materials should be addressed to

m.towers@sheffield.ac.uk

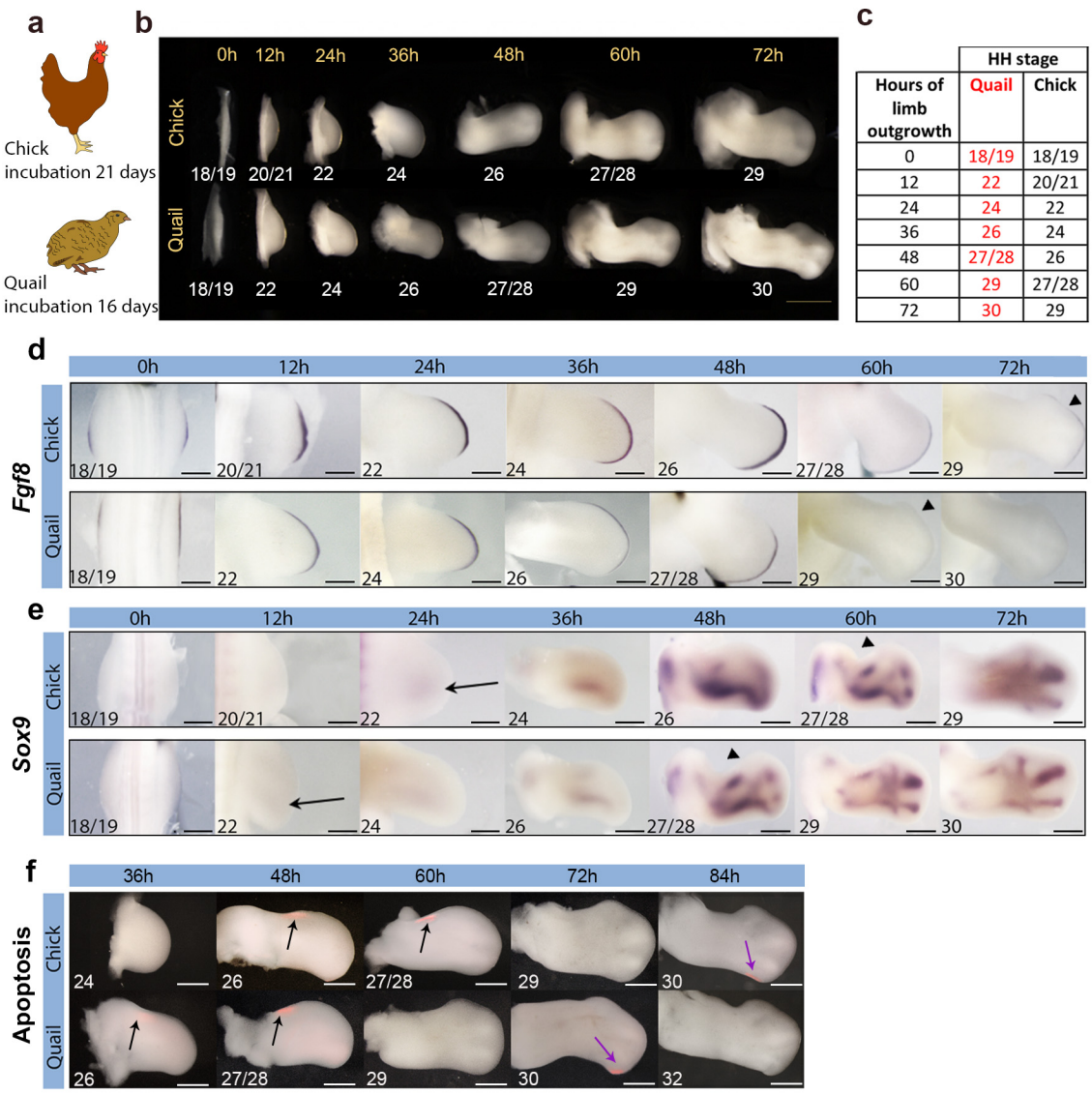

Hours of limb outgrowth	HH stage Quail	HH stage Chick
0	18/19	18/19
12	22	20/21
24	24	22
36	26	24
48	27/28	26
60	29	27/28
72	30	29

Figure 1. Developmental timing is accelerated in quail wing buds

(a) Schematics of the chick and quail that have 21- and 16-day incubation periods, respectively. **(b, c)** Hamburger Hamilton (HH) staging of chick and quail wings over 72 hours until HH29 and HH30, respectively - 0-hour refers to day 3 of incubation. (**d**) The apical ectodermal ridge marker, *Fgf8,* is down-regulated at HH29 - 72 hours in the chick wing and 60 hours in the quail wing, indicated by arrowheads. HH stage noted in the bottom left corner **(e)** Cartilage differentiation indicated by *Sox9* is 12 hours advanced in the quail wing compared to the chick (compare 48-hour quail wing and 60-hour chick wing - arrowheads). Black arrows indicate the

onset of *Sox9* expression at HH22. **(f)** Anterior (black arrows) and posterior (purple arrows) necrotic zones (red) are 12 hours advanced in quail wings compared to chick wings (*n* =4). Scale bars: a – 1mm, d – 12h, 24h -200µm; 36h -400µm; 0h, 48h, 60h -500µm; 72h -600µm. e – 12h, 24h -250µm; 0h -400µm; 36h -500µm; 48h, 60h -600µm; 72h -700µm. f – 36h, 48h, 60h -500µm; 72h -600µm, 84h -750µm.

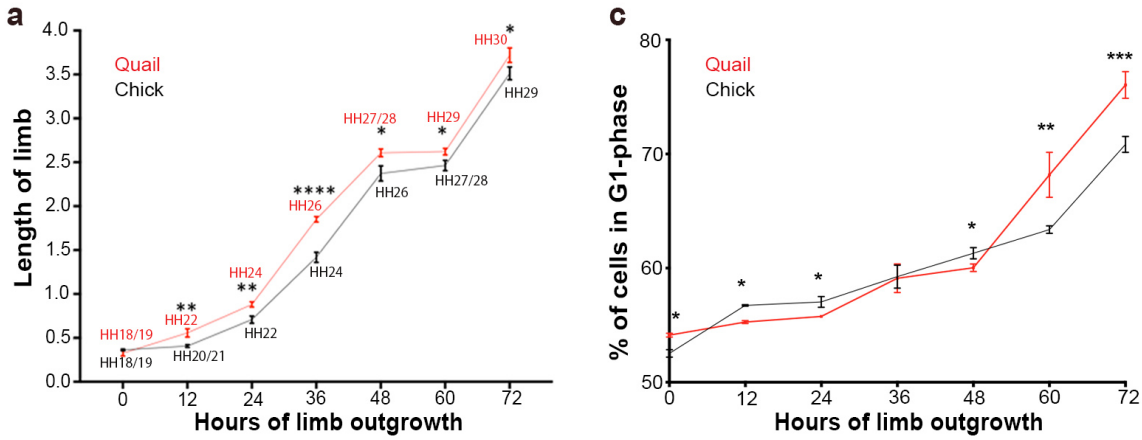

b

Days of limb outgrowth	Quail Length (cm)	Chick Length (cm)	Fold difference
HH22	0.0557	0.0708	1.27
HH29	0.26	0.35	1.35

Figure 2. Growth rates are equivalent in quail and chick wings and are uncoupled from HH stage progression

(a) Proximo-distal lengths of quail and chick wings buds (body wall to tip of wing bud) are not significantly different at 0 hours, but are significantly different between 12 and 72 hours, indicated by student *t*-tests (12h *p*-value = 0.0017, 24h *p*-value =0.0079, 36h *p*-value =<0.0001, 48h *p*-value =0.0382, 60h *p*-value =0.0280, 72h *p*-value =0.0268). Quail wings grow at a significantly faster rate between 0-12 hours, as determined by student *t*-test (*p*-value = 0.0462) (*n*=4). However, there is no significant difference in incremental changes in growth rates from 12-72 hours as determined by Wilcoxon tests (*p*-value = 0.688 - *n*= 4-14). **(b)** Average lengths of quail and chick wings, and fold differences at HH22 and HH29. **(c)** The proportion of distal mesoderm cells in G1-phase indicates that the quail has a significantly faster cell cycle at 12 hours (*p*-value =0.0165) 24h (*p*-value =0.0144) and 48h (*p*-value = 0.0175), and the chick at 0h (*p*-value = 0.0123), 60h (*p*-value = 0.0018) and 72h (*p*-value =0.0004). Student *t*-tests were

performed on *n*=3 repeats of 8-12 pooled blocks of distal mesenchyme. *p*-values: *=<0.05, **=<0.01 ***= <0.001 ****= <0.0001.

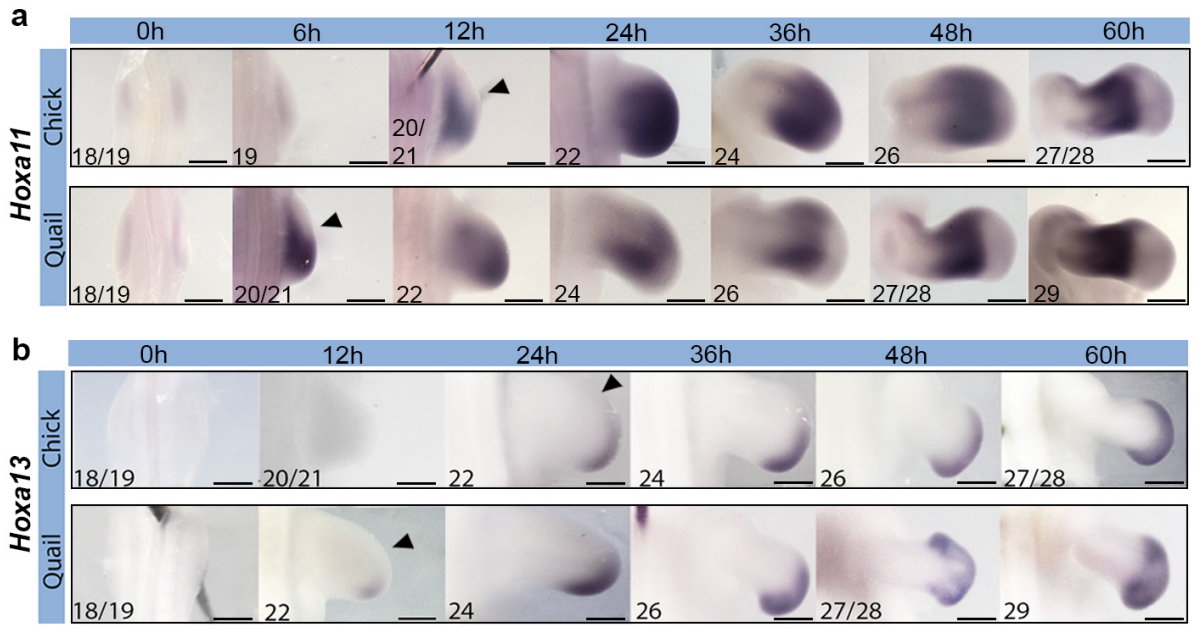

Figure 3. Proximo-distal specification is faster in quail wing buds

(a) *Hoxa11* is expressed at HH20/21, which is 6 hours earlier in quail compared to chick, arrowheads indicate onset of expression, HH stage noted in the bottom left corner. **(b)** *Hoxa13* is expressed at HH22, which is 12 hours earlier in quail compared to chick, arrowheads indicate onset of expression.

Scale bars: a – 6h, 12h, 24h - 300µm; 0h, 36h - 500µm; 48h, 60h - 600µm; b – 12h, 24h - 200µm; 0h, 48h chick - 300µm; 36h - 400µm, 48h quail - 600µm, 60h - 800µm.

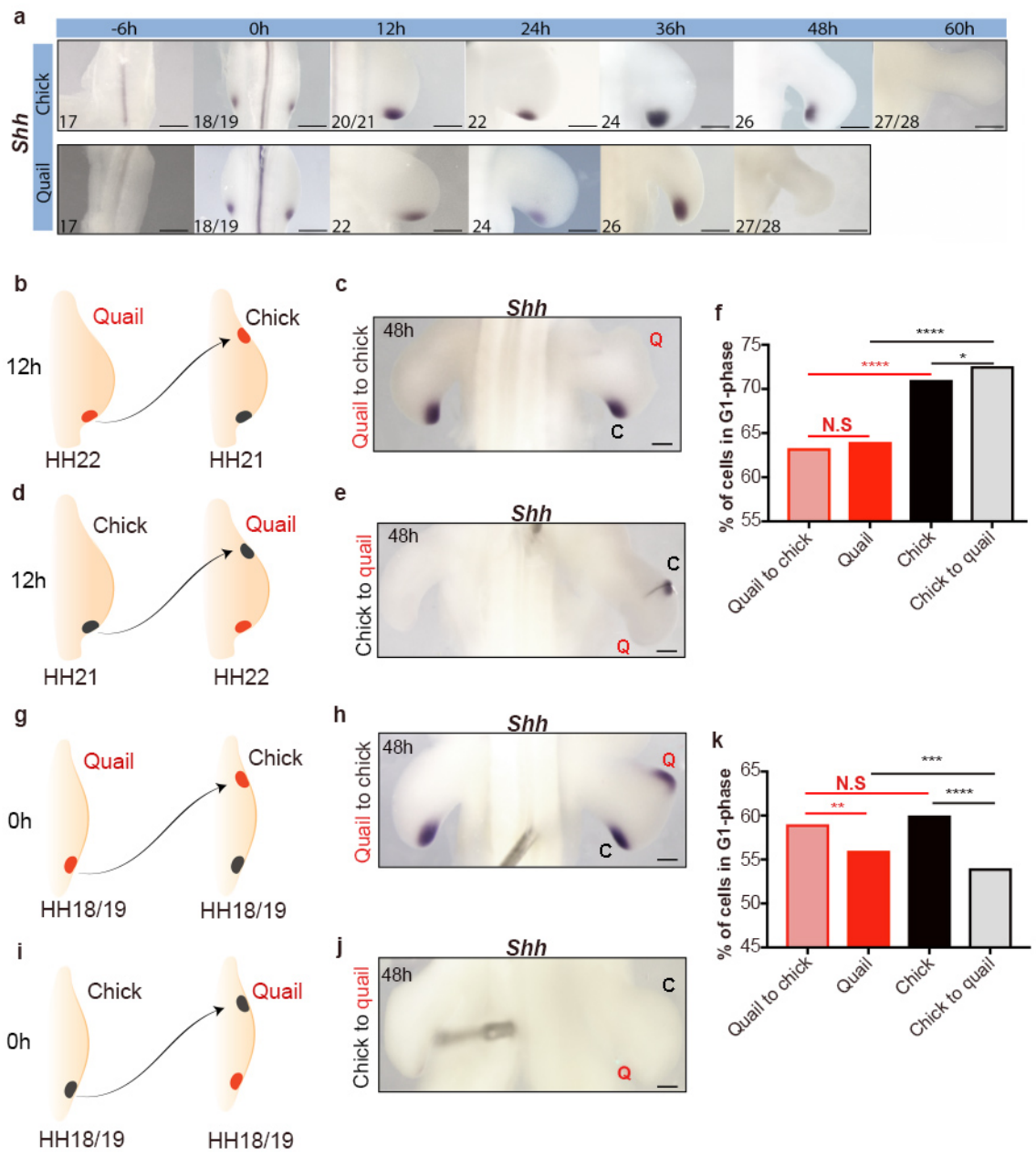

Figure 4. Resetting potential of species developmental timing in polarising region grafts

(a) *Shh* is expressed 12 hours longer in chick wings compared to quail wings until HH26 (HH stage noted in the bottom left corner). In interspecies polarising region grafts between 12-hour quail (HH22) and chick (HH21) wings (made to the anterior margins of host wing buds) **(b, d),** *Shh* expression is maintained according to donor timing **(c** n=5/6, **e** n=3/5). **(f)** Cell cycle parameters in grafts are close to donor values but are significantly different from the host polarising region 24 hours after the graft was performed (Pearson's χ^2 test) p-values = quail vs.

quail grafted to chick = 0.24, chick vs. quail grafted to chick = 0.00001, chick vs. chick grafted to quail = 0.013, quail vs. chick grafted to quail = 0.00001. In interspecies polarising region grafts between 0-hour quail and chick wings (HH18/19 in both species) **(g, i)**, *Shh* expression is reset according to host timing **(h**, *n*=6/6, **j** n=3/5). **(k)** Cell cycle parameters in grafts are reset close to host values 24 hours after the graft was performed. (Pearson's χ^2 test) *p*-values = quail vs. quail grafted to chick = 0.02, chick vs. quail grafted to chick = 0.09, chick vs. chick grafted to quail = 0.00001, quail vs. chick grafted to quail = 0.00012. *p*-values – N.S = >0.05 ***= <0.001 ****= <0.0001.

Scale bars: a- 12h, 24h - 300µm; 36h - 500µm; -6h, 0h, 48h, 60h - 600µm; 48h quail - 700µm. c, e, h, j - 500µm

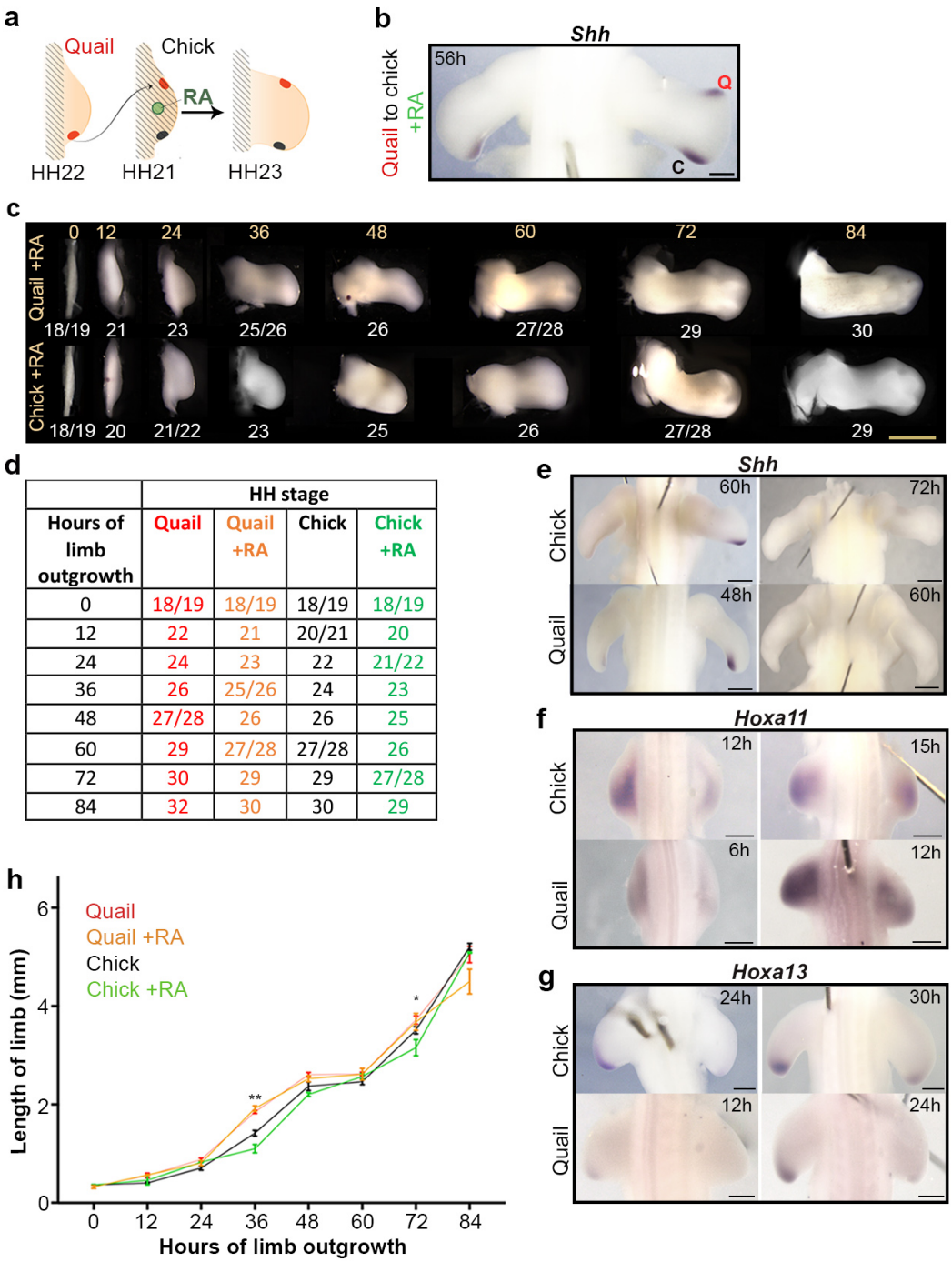

	HH stage			
Hours of limb outgrowth	Quail	Quail +RA	Chick	Chick +RA
0	18/19	18/19	18/19	18/19
12	22	21	20/21	20
24	24	23	22	21/22
36	26	25/26	24	23
48	27/28	26	26	25
60	29	27/28	27/28	26
72	30	29	29	27/28
84	32	30	30	29

Figure 5. Retinoic acid can set species developmental timing and rescale patterning

(a) HH19 chick wings were treated with retinoic acid-soaked beads (green circle), and at 12 hours (HH21) received polarising regions grafts from 12-hour quails (HH22); note, black hatching indicates retinoic acid. **(b)** *Shh* expression is prolonged until approximately 56 hours in both the host and donor (n=3/4). **(c, d)** HH stages of chick and quail wing buds treated with

retinoic acid at 0 hours, compared with the contralateral untreated wing. **(e)** Retinoic acid-treated wings express *Shh* until 60 hours in the chick (*n*= 4/4) and 48 hours in the quail (*n*=3/3), compared to 48 and 36 hours in control untreated. **(f)** Retinoic acid-treated wings express *Hoxa11* at 15 hours in the chick (*n*=3/5), and 12 hours in the quail (*n*=3/5), compared to 12 and 6 hours in control untreated. **(g)** Retinoic acid-treated wings express *Hoxa13* at 36 hours in the chick (*n*=3/4) and 24 hours in the quail (*n*=3/5), compared to 24 and 12 hours in control untreated wings. **(h)** Proximo-distal lengths of quail and retinoic acid-treated quail wings (Quail +RA) are not significantly different throughout outgrowth; chick and retinoic acid-treated chick wings (Chick +RA) are also not significantly different except at 36 hours (*p* - value = 0.0196) and 72 hours (*p*-value =0.0419), indicated by student *t*-tests. Wilcoxon tests reveal no significant difference in incremental growth rates between chick vs. chick +RA, chick vs. quail +RA, chick +RA vs. quail, quail vs. quail +RA, and chick +RA vs. quail +RA (*p* - values = >0.99, >0.99, 0.563, 0.438, 0.688 respectively). For chick vs. quail see Figure 1d. *n*= 4-8. *p*-values: *=<0.05, **=<0.01

Scale bars: b - 500µm; d, - 1mm; f - 400µm, g, h –250µm,

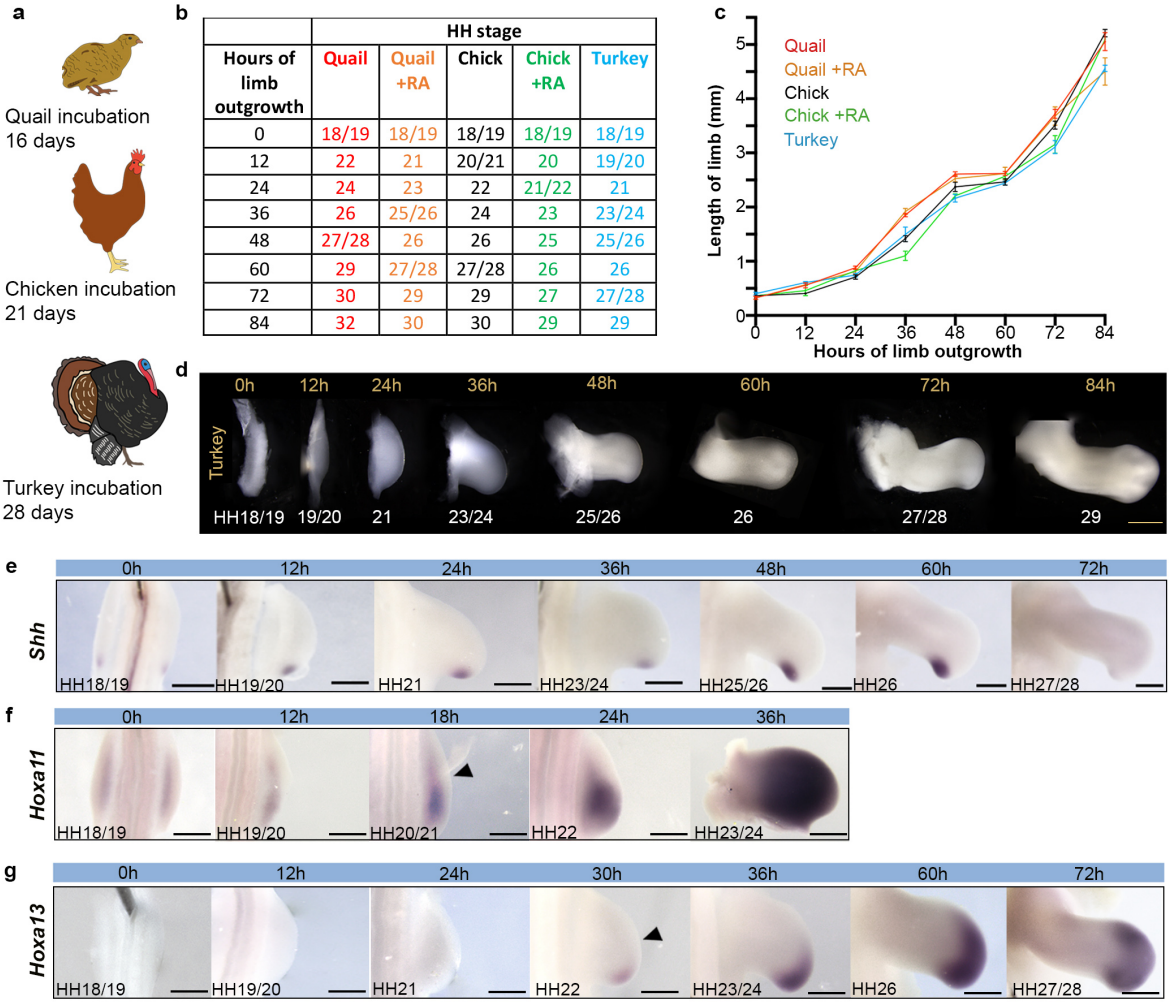

Hours of limb outgrowth	HH stage: Quail	Quail +RA	Chick	Chick +RA	Turkey
0	18/19	18/19	18/19	18/19	18/19
12	22	21	20/21	20	19/20
24	24	23	22	21/22	21
36	26	25/26	24	23	23/24
48	27/28	26	26	25	25/26
60	29	27/28	27/28	26	26
72	30	29	29	27	27/28
84	32	30	30	29	29

Figure 6. Retinoic acid treated chick wings replicate turkey developmental timing and pattern scaling

(a) Schematics of quail, chick and turkey that have 16, 21 and 28-day incubation periods, respectively. **(b,d)** HH staging of turkey wings over 84 hours until HH29 - 0-hour refers to day 4 of incubation. **(c)** Proximo-distal lengths of quail, quail +RA, chick, chick +RA and turkey wings buds until 84 hours (HH29 in turkey and chick +RA wings). Wilcoxon tests reveal no significant difference in incremental growth rates between turkey vs. chick +RA, turkey vs. quail +RA, turkey vs. quail and turkey vs. chick (p -values = >0.437, >0.99, 0.563, 0.219, respectively). n= 4-8). **(e)** *Shh* is downregulated at HH26, HH stages noted in the bottom left

of each panel. **(f)** *Hoxa11* is expressed at HH20/21, arrowheads indicate onset of expression, and **(g)** *Hoxa13* is expressed at HH22, arrowheads indicate onset of expression. *p*-values: *=<0.05, **=<0.01 ***= <0.001 ****= <0.0001.

Scale bars: d - 750µm; e - 500µm, f- 0-36h - 500µm, 60h, 72h - 600µm 0h, 24h - 400µm, 12h, 36h-72h- 500µm

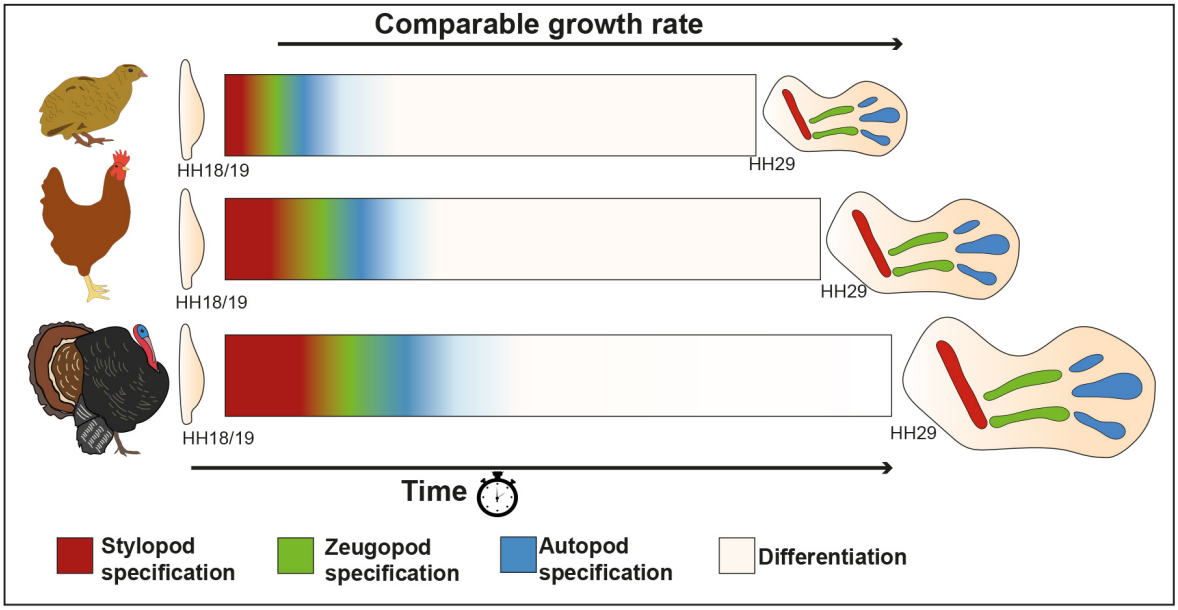

Figure 7. Developmental timing scales avian wing patterning

Schematics depicting the timing of proximo-distal specification and differentiation in avian wings (quail, chick and turkey) from HH18 until the end of the patterning phase at HH29, when the skeletal elements have been laid down. In this model, the stylopod (red) is specified by high levels of retinoic acid signalling; intermediate specification of the zeugopod (green) by low levels retinoic acid signalling at HH20/21 and autonomous timing, and distal specification of the autopod (blue) triggered by an autonomously timed epigenetic mechanism and the loss of retinoic acid signalling at HH22. The duration of proximo-distal specification varies between species, however the duration of differentiation (white) remains relatively constant. Thus, the timing of proximo-distal specification and differentiation alongside a comparable growth rate scales pattern formation between species. Consequently, at HH29 there is a 1.34-fold difference in the size of the quail and chick wings, a 1.31-fold difference in the size of chick and turkey wings, and a 1.81-fold difference in the size of quail and turkey wings – schematics of HH29 wings are proportionately scaled.